Studies on the application of n-InGaZnO/p-Si heterojunctions in active pixel sensor as photodiode

GUOLIANG ZHANG, YUN ZENG*, YONGMING YAN, YONGQING LENG
School of Physics and Microelectronics Science, Hunan University, Changsha, 410082, People's Republic of China

Photodiodes based on n-InGaZnO/p-Si heterojunction have been fabricated by radio frequency magnetron sputtering of n-IGZO films on p-type Si(100) substrates. Based on the current-voltage (I-V) characteristics and capacitance-voltage (C-V) characteristics measured under various incident light powers (ILP), we explained them and their effects on the application of IGZO/Si heterojunction in active pixel sensor (APS) as photodiode (PD). It is indicated that IGZO/ Si heterojunction shows much more advantages such as higher quantum efficiency (QE) and dynamic range (DR) and better adaptability to low power supply voltage than the commonly used Si n-p PD due to its nonlinear light I-V and C-V characteristics.

(Received February 05, 2013; accepted July 10, 2014)

Keywords: Photodiode, APS, Dynamic range, Low power supply voltage

1. Introduction

In recent years, various types of transparent oxide/Si heterostructure such as ZnO/Si, AZO/Si and IGZO/Si are used as photodetectors [1-3]. The general idea is to cover the light absorption material Si with oxide material which is transparent in the visible region, therefore, the photoabsorption occurs mainly at the depletion region of Si substrate and the photo induced electron is swept through the junction to achieve high quantum efficiency (QE) [4,5]. The transparent oxide/Si heterojunction shows many advantages such as high QE, uniform spectral responsivity, low deposition temperature and compatible with the traditional silicon semiconductor technology [6-8]. However, so far as we known, there hasn't been any discussion about the effects of the common nonlinear light I-V and C-V characteristics on application as PD in image sensor [9]. And it limits the promising application of transparent oxide/Si heterojunction in image sensor.

The present paper is based on a study to use an amorphous n-IGZO film deposited on p-Si (100) substrate to form heterojunction. Because the amorphous IGZO has a wide band gap of approximately 3.2 eV [10], low energy photons in the visible range are mainly collected at the depletion region of Si substrate, therefore extremely high QE (82%) is achieved. And besides, because there is an amorphous oxide layer (~2.5 nm thick) formed at the transparent oxide/Si interface during deposition [11], the light I-V characteristics of IGZO/Si PD shows S-shaped curves which is also observed in ZnO/Si and AZO/Si PD. Furthermore, the light C-V measurement was done and the results show that the C-V characteristics were also affected by the amorphous oxide interface layer. Here, we discussed the application of IGZO/Si heterojunction in APS, which is the most commonly used image sensor due to its low power consumption and flexible functions [12,13]. Since the performance of APS is mainly determined by the I-V and C-V characteristics of the applied PD, it is predictable that the nonlinear characteristics of IGZO/Si PD show significant effects on its application in APS.

2. Experimental

The details of experiment process have been reported in our earlier work [3], in brief, P-type Si (100) (5~20 Ω cm) wafer was chosen as the substrate, an Al film was deposited onto the backside of Si substrates to form ohmic contacts. Before being deposited IGZO film on, an approximately 3nm thick SiO_2 buffer layer was grown on the surface of Si substrates by electron beam evaporation to restrain the surface oxidation during the next step. Then, n-IGZO was deposited on SiO_2/Si substrates at room temperatures, the ratio of Ar/O_2 flow was fixed to 12:2. The size of IGZO film is 2×3 ㎜^{2}, and the carrier concentration is 1.2×10^{17} cm^{-3} from Hall measurement. For ohmic contact to the n-IGZO film, an 2×3 ㎜^{2} Indium tin oxide (ITO) film was deposited on the IGZO surface.

At first, we studied the effect of ILP on the I-V, C-V characteristics and performances of the devices by delivering a red laser beam (636 nm wavelength) with various powers (from 1 mW/cm^2 to 50 mW/cm^2) on the surface of samples, and then explained these characteristics according to our theoretical model with IL considered which we reported earlier. Furthermore, a 200 W xenon-arc lamp was used as the light source for the spectral responsivity study in the range of 300 to 800 nm

with a monochrometer. All the measurements were taken at room temperature (25 ℃). Based on the experimental data, we also studied the effects of the nonlinear I-V and C-V characteristics of IGZO/Si heterojunction on its application in APS as PD.

3. Results and discussion

The schematic diagram of a most commonly used APS is plotted in the inset of Fig. 1. At first, the voltage of node A is initialed to the power supply voltage V_{dd}, after that, the reset field-effect transistor (FET) M1 is shutoff and the light integral process starts, photocurrent generated in PD charges the capacitance at node A thus reduces the voltage. Therefore, the intensity of incident light P_I is transformed to the magnitude of voltage drop. Since the gate capacitance of FET M2 is negligible comparing to the capacitance of IGZO/Si PD, the I-V characteristic of IGZO/Si PD together with the C-V characteristic play important roles during the light integral process.

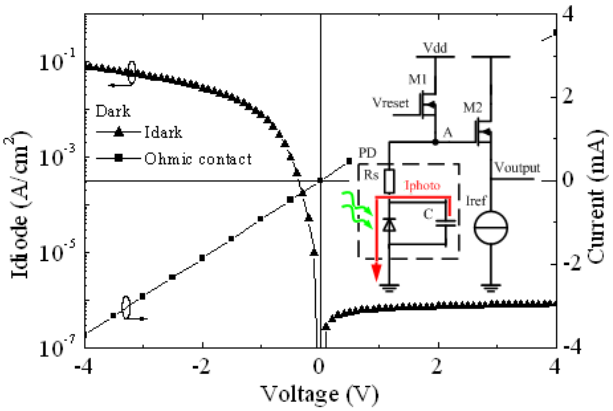

Fig. 1. I-V curve of the ITO/IGZO/SiO_2/p-Si/Al heterojunction PD in dark. Inset shows the schematic diagram of APS.

A. I-V characteristics

Fig. 1 shows the current-voltage characteristic of the ITO/IGZO/SiO_2/p-Si heterojunction measured at room temperature in the dark. The ohmic contacts of ITO on IGZO layers are confirmed by the good linear I-V dependences, I-V curves of devices show rectifying behaviors.

The most important characteristic of IGZO/Si PD, light I-V characteristic was measured under various ILPs. As shown in the inset of Fig. 1, since the series resistance is independent from the light integral process, the value of series resistance (~870 Ω) is already found out by using Thomas L. Paoli's analog derivative technique [14], photoresponsivity versus the reverse voltage bias (RVB) with series resistance eliminated are plotted in Fig. 2.a. According to our theoretical model, the inherent S-shaped light I-V characteristic of IGZO/Si PD is caused by the low electron mobility and deficiency of conduction electrons at IL which leads to electron accumulation at IL thus enhancing the electron recombination in IL and space-charge region (SCR) of Si. The shape of light I-V curves depends on the carrier conduction power of IL, amount of charged interface states and majority carrier concentration of IGZO film N_{igzo}, and that of Si substrate N_{si}. With increasing ILP, more interface states are negatively charged by photo-induced electrons thus generate larger photocurrent, however, it also results in higher electron quasi-Fermi level at IL, larger partial voltage on SCR of IGZO, and thereby enhancing the electron recombination in SCR of Si. Therefore, the reverse voltage bias photocurrent saturates at V_s is higher. For comparison, I-V curves were calculated according to our theoretical model and plotted in Fig. 2.b, it is obvious that this theoretical model agrees with the experimental data generally well. However, when P_I drops below 2 mW/cm^2, the measured V_s settles at 1.42 V while that according to our model keeps lowering. As P_I decreases, the amount of occupied interface states is smaller and consequently the electron quasi-Fermi level at IL drops. Since the value of V_s varies in inverse proportion to the conduction power of IL, the constant measured V_s under weak ILP may caused by poor conduction power of electrons at low energy interface state, which is reasonable since more energy is needed for these electrons to enter conduction band.

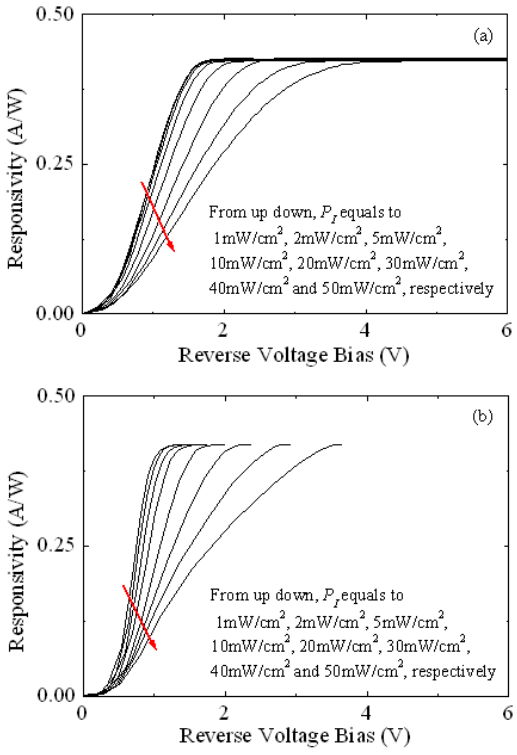

Fig.2. (a) Experimental photoresponsivity of IGZO/Si PD under different ILPs. (b)Theoretical photoresponsivity under different ILPs.

The photocurrent versus ILP curves under different RVBs are plotted in Fig. 3, the photocurrent increases linearly with increasing ILP under RVBs higher than 5 V while this relationship is changed under lower RVBs, the photocurrent increases less with increasing ILP thus leads to nonlinear photoresponsitivity. APS is the most affected image sensor since the RVB on the PD keeps changing during the light integral period.

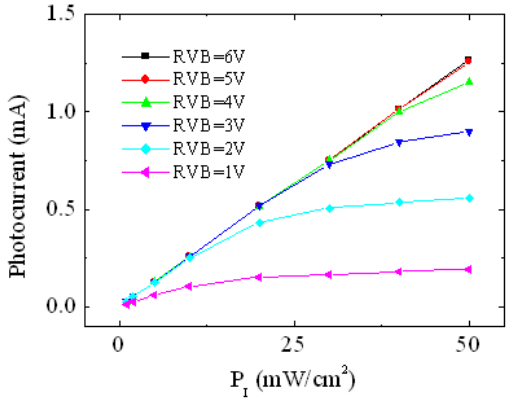

Fig. 3. Photocurrent versus ILP under different RVBs.

The spectral responsivity are plotted in Fig. 4, the spectral responsivity is quite uniform over the range of visible light (400 nm to 800 nm), under 5V RVB, the highest quantum efficiency of 83 % was obtained under 620 nm photons with the responsivity of 0.42 A/W. When the wavelength of incident light decreases to 320nm, the QE drops to 0.8 % sharply, the photons with energy higher than the ITO electrode band gap (3.7 eV, ~330 nm) aren't able to penetrate the ITO film, therefore, the photoresponsivity in the ultraviolet region is quite low. The spectral responsivity of IGZO/Si PD is close to that of human eye and the high responsivity of 0.35 A/W at 570 nm allows further development with additional filter [15,16]. Because the photocurrent saturates near 5 V of reverse bias, the responsivity varies little with RVB increases from 5 V to 10 V. However, the decrease of responsivity under low RVB as shown in Fig. 3 also appears in the spectral responsivity curves, as the RVB decreases to 1 V, the responsivity and QE under 570 nm photons drop to 0.17 A/W and 39 %, respectively.

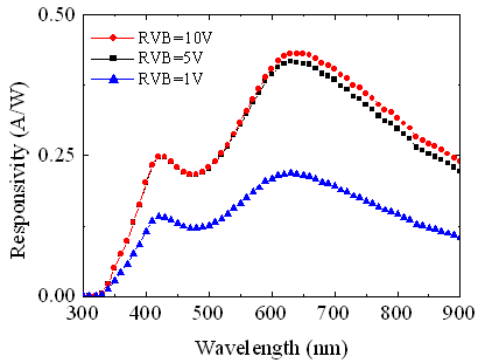

Fig. 4. Spectra responsivity under the RVBs of 1, 5 and 10 V.

B. C-V characteristics

The C-V measurements were done below 10 kHz under various ILPs and the reciprocal of the capacitance squared versus RVB are plotted in Fig. 5. Different from C^{-2}-RVB characteristic of Si n-p PD that of IGZO/Si PD shows special L-shaped curves which is actually familiar in many heterostructure [17,18]. Our model is used to explain this phenomenon; voltage division of IGZO/Si heterojunction diodes under ILP of 10 mW/cm^2 is calculated as in Fig. 6. It is clearly seen that, before the photocurrent saturates, the increase of applied reverse voltage is almost on the SCR of IGZO, therefore, the rate of slope of C^{-2}-RVB curves is mainly determined by the carrier concentration of IGZO, after that, the interface layer no more shows effects on the voltage division, same as Si n-p PD, the voltage division agrees with the following equation

$$\frac{dV_{igzo}}{dV_{Si}} = \frac{\varepsilon_{Si} N_{Si}}{\varepsilon_{igzo} N_{igzo}} \tag{1}$$

and the rate of slope of C^{-2} is given by

$$\frac{dC^{-2}}{dV} = \frac{2\left(\varepsilon_{Si} N_{Si} + \varepsilon_{igzo} N_{igzo}\right)}{q\varepsilon_{Si}\varepsilon_{igzo}\varepsilon_0 N_{Si} N_{igzo}} \tag{2}$$

where ε_0 is the permittivity of vacuum, ε_{Si} and ε_{igzo} are the relative permittivity of Si and IGZO, respectively, and q is the electronic charge. Accordingly, N_{igzo} and N_{si} are then calculated from experimental data as 9.5×10^{16} and 1.8×10^{15} cm^{-3}, respectively, and these values are close to what we got from Hall measurement which are 1.2×10^{17} and 1.4×10^{15} cm^{-3}. Therefore, the whole C^{-2}-RVB characteristic of IGZO/Si PD is reflected in L-shaped curves, the rate of slope of the low RVB regions is determined by N_{igzo} and the other is mainly determined by N_{si}.

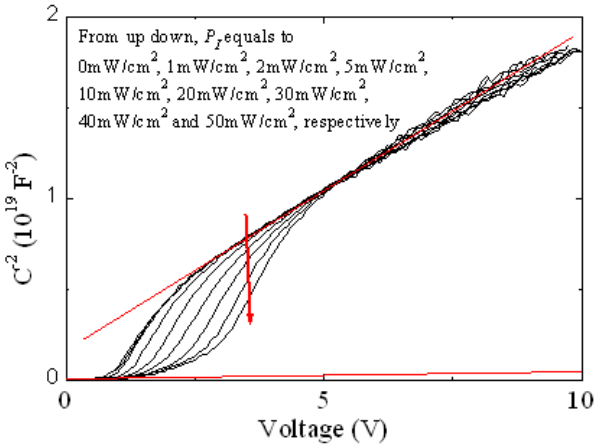

Fig. 5. Experimental reciprocal of the capacitance squared versus RVB under different ILPs.

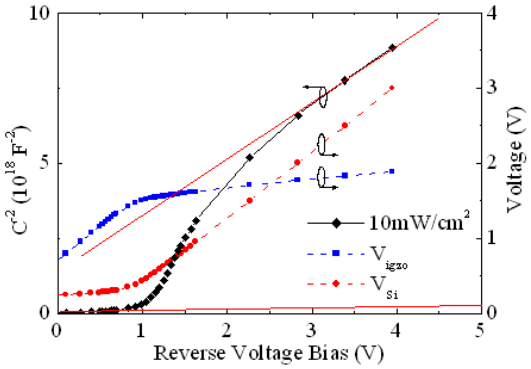

Fig. 6. Theoretical reciprocal of the capacitance squared and voltage division versus RVB under incident light of 10 mW/cm^2.

C. Application in APS and discussion

According to the structure of APS, the photocurrent is integrated at the capacitance of IGZO/Si PD by charging it during the integral period, after that, P_I is reflected in the magnitude of voltage drop at node A which is given by

$$V_{signal} = \int_0^{t_i} I_{photo}/C_{photo}\, dt \qquad (3)$$

where t_i is the light integral period, I_{photo} the photocurrent and C_{photo} the corresponding light capacitance. After the reset FET M1 is shutoff, the light integral process occurs in a simple closed system. Only the I-V and C-V characteristics of IGZO/Si PD, the source capacitance of FET M1 and the gate capacitance of FET M2, the latter two capacitances are negligible comparing with the first one, are included in this system. Thus, simulation is quite suitable for the studies on the application of IGZO/Si heterojunction in APS, MATLAB is used to solve equations and most of the noises such as thermal noise, reset noise are neglected.

At first, we discussed the situation of 5 V initial voltage with 10 μs integral period, which are common parameters in APS [19]. The voltage at node A V_A during the integral period is plotted in Fig. 7.a. As shown in picture, the light integral process shows clear difference when P_I exceeds 10mW/cm^2. With increasing P_I, V_A drops faster, however, as shown in Fig. 7.b, I_{photo}/C_{photo} also decreases as V_A approaching ground voltage thus slows the voltage drop speed, which consist a negative feedback in the light integral process. Therefore, the voltage drop at node A under strong ILP is depressed and its value is much lower than that of voltage drop in the case of APS using Si n-p PD. Under weak ILP below 5 mW/cm^2, V_A drops slightly and keeps higher than the corresponding V_s, the S-shaped I-V characteristic and the L-shaped C^{-2}-V characteristic shows few effects on the light integral process. Thereby, I_{photo}/C_{photo} almost keeps constant during the integral period under weak ILP, and the voltage drop at node A for IGZO/Si PD shows no difference from that for Si n-p PD. This characteristic helps enlarging the maximum detectable ILP as keeping the minimum detectable ILP constant.

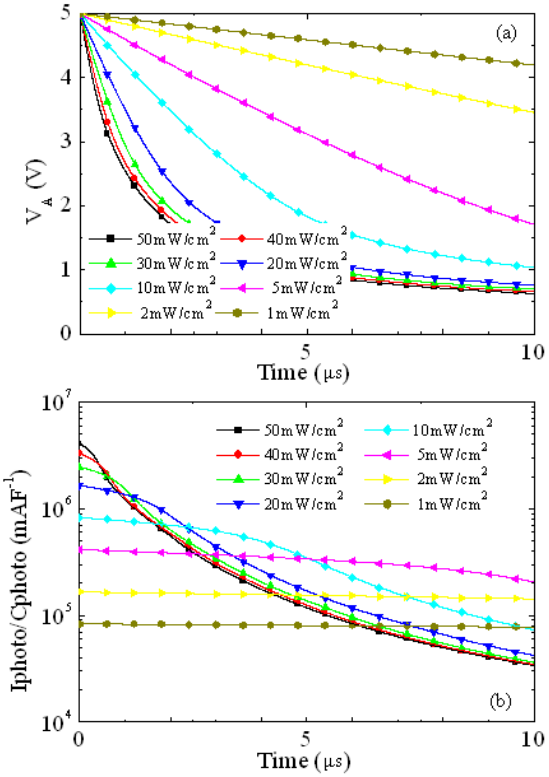

Fig. 7. (a) The voltage at node A during the light integral period. (b) I_{photo}/C_{photo} during the light integral period.

Furthermore, because the trend of development in APS is low power supply voltage and IGZO/Si PD shows potentialities in detecting strong light signal, it is valuable to discuss the application of IGZO/Si PD under lower power supply voltage [20]. As shown in Fig. 8, the value of initial voltage is in ranged from 5 V to 1 V, V_{signal} is correspondingly decreased under lower power supply voltage. Since the threshold voltage of MOSFET is constant and independent from power supply voltage, the effective lower limit voltage at node A is determined by read out circuit, its value usually equals to that of the threshold voltage of FET M2 in the inset of Fig. 1. Assuming lower limit voltage at node A equals to 0.7 V, the red line in Fig. 8 visually represents the maximum voltage drop, under which the incident light signal is detectable. It is clear that, under lower power supply voltage, the maximum intensity of detectable signal is decreased. The voltage drop at node A of APS using Si n-p PD under ILP of 5 mW/cm^2 is also plotted in Fig. 8, it is obvious that, with the same maximum limit of intensity of incident light decided, 5 mW/cm^2 for example, IGZO/Si PD is able to work under lower power supply voltage, 4.17 V for Si PD and 0.86 V for IGZO/Si PD, respectively. The same trend is also shown as the power supply voltage decreases. When the power supply voltage drops from 5 V to 1 V, the maximum intensity of detectable incident light is 30.1 mW/cm^2, 27.1 mW/cm^2, 22.4 mW/cm^2, 18.2 mW/cm^2 and 8.1 mW/cm^2 for IGZO/Si PD and 6.0 mW/cm^2, 4.8 mW/cm^2, 3.6 mW/cm^2, 2.2 mW/cm^2 and 0.6 mW/cm^2 for Si PD. It is indicated that with power supply

voltage fixed, the maximum intensity of detectable incident light is much higher in the case of IGZO/Si PD than Si PD. As conclusion, IGZO/Si PD is able to detect much stronger incident light than Si PD and is more suitable to work under low power supply voltage.

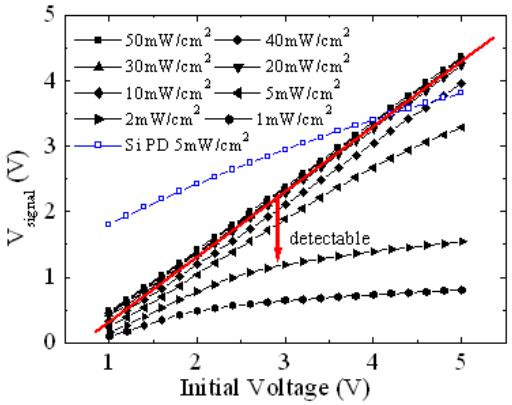

Fig. 8. The voltage drop at node A versus initial voltage, light integral period is fixed to 10 μs. Voltage drop at node A of APS using Si n-p PD under 5 mW/cm² incident light is plotted as comparison.

Since the light integral process behaves like a low-pass filter and is able to eliminate high frequency noises, the minimum detectable photocurrent is mainly caused by the non-uniform dark leakage current I_{dl} (~0.7 μA/cm²). According to the light I-V characteristics, I_{dl} shows no visible increase with increasing P_I, it is reasonable to assume that I_{dl} keeps constant under different ILPs. Furthermore, as the capacitance of PD keeps increasing as RVB decreases, the magnitude of noise voltage is determined by both P_I and the capacitance of IGZO/Si PD. The voltage drop caused by I_{dl} is given by

$$V_{noise} = \int_0^{t_i} I_{photo}/C_{photo}\,dt - \int_0^{t_i} \left(I_{photo} - I_{dl}\right)/C_{photo}\,dt \quad (4)$$

As shown in Fig. 9, V_{noise} is much lower as P_I increases due to larger average C_{photo} during the light integral period. After the calculation of V_{noise}, the intensity of the noise equivalent power (NEP) caused by I_{dl} is given by

$$P_{noise} = P_I V_{noise}/V_{signal} \quad (5)$$

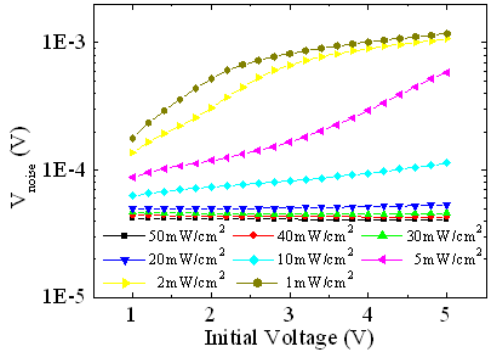

Fig. 9. The voltage drop caused by I_{dl} versus initial voltage under different ILPs, light integral period is fixed to 10 μs.

As shown in Fig. 10, the magnitude of NEP is larger due to lower signal noise rate as initial voltage drops while this trend is much slighter when the intensity of incident light is below 10 mW/cm², it helps keeping the noise signal uniform across the entire sampled picture.

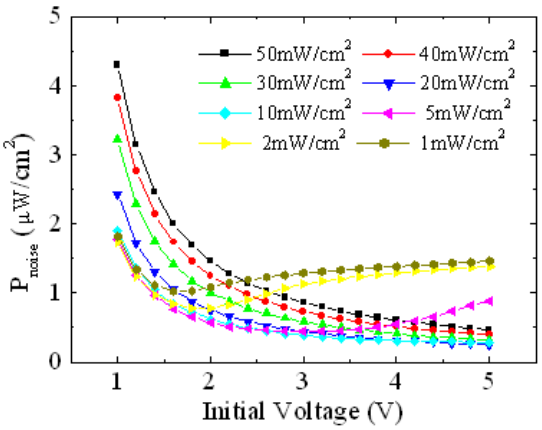

Fig. 10. NEP versus ILP with various initial voltages, light integral period is fixed to 10 μs.

Therefore, as application in APS, the minimum detectable ILP P_{min} is the same in the cases of n-IGZO/p-Si PD and Si n-p PD while the maximum detectable ILP P_{max} of n-IGZO/p-Si PD is significantly stronger. Dynamic range is the most important parameter of an APS [21], which is given by

$$DR = 20\lg\left(P_{\max}/P_{\min}\right) \quad (6)$$

it is predictable that the DR of IGZO/Si PD should be much higher. To calculate its value, three situations are considered; first, 10 μs integral period with 0.7 V lower limit voltage, second, 30 μs integral period with 0.7 V lower limit voltage and third, 30 μs integral period with 0.4 V lower limit voltage. As shown in Fig. 11, the DR of APS using n-IGZO/p-Si PD is much higher than that of APS using Si n-p PD and this trend is more obvious with shortening integral period, reducing lower limit voltage at node A or lowering power supply voltage. For example, as integral period decreases from 30 μs to 10 μs with lower limit voltage of 0.7 V, the maximum increase of DR is 15 dB for IGZO/Si PD and 10 dB for Si PD, respectively, and these values are 21 dB and 5 dB, respectively, as the lower limit voltage at node drops from 0.7 V to 0.4 V. It is indicated that the reduction of lower limit voltage at node A is much more effective than shortening light integral period on increasing DR. And as shown in situation 3, the difference between the DR of IGZO/Si PD and that of Si PD is 23.7 dB under 5 V power supply voltage, however, this value increases to 34.8 dB under 1 V power supply voltage. As conclusion, IGZO/Si PD is more suitable for the application under low power supply voltage, and this advantage is much more significant with lowering the lower limit voltage at node A or shortening the period of light integral process.

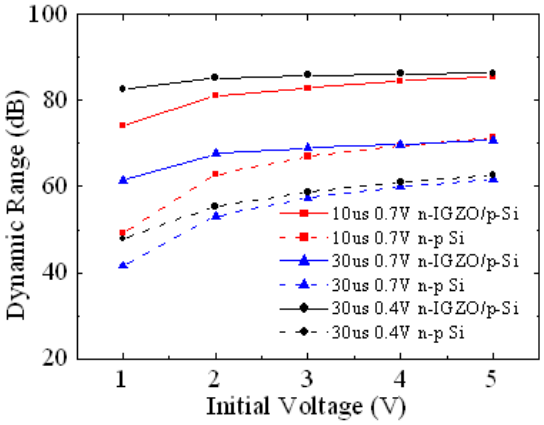

Fig. 11. Comparison of the DRs of APS using IGZO/Si PD and Si PD in situations of different light integral periods and lower limit voltages.

4. Summary and conclusions

In summary, IGZO/Si PD fabricated here shows extremely high QE (82 %) and uniform spectral resonsivity over the range of visible light. Furthermore, intensity of incident light has effects on both the light I-V and C-V characteristics of n-IGZO/p-S heterojunction by affecting the amount of charged interface states and the division of RVB. These effects directly affect the application of IGZO/Si PD in APS by decreasing the conversion gain under strong ILP. Since the NEP only shows slight change with increasing the intensity of incident light or decreasing power supply voltage, the minimum detectable ILP keeps constant while the maximum detectable ILP is enlarged. Due to the nonlinear photoresponsivity and C^{-2}-V characteristic, IGZO/Si PD actually has higher DR and this advantage is much more significant as working under low power supply voltage than Si PD. The studies indicate that IGZO/Si PD shows better performances and more potentiality under low operation voltage than traditional Si PD as application in APS, which would leads to more flexible APS design.

Acknowledgments

This work was supported by the National Natural Science Foundation of China (61350007) and the Project supported by Hunan Provincial Natural Science Foundation of China (11JJ2034).

References

[1] S. Mridha, D. Basak, JAP. **101**, 083102 (2007).
[2] Ju-Hyung Yun, Joondong Kim, Materials Letters. **70**, 4 (2012).
[3] Guoliang Zhang, Yun Zeng, YongMing Yan, J. Optoelectron. Adv. Mater. **5**, 1011 (2011).
[4] X. L. Xu, S. P. La, J. S. Chen, Cryst. Growth **223**, 201 (2001).
[5] E. A. Douglas, A. Scheurmann, R. P. Davies, Appl. Phys. Lett. **98**, 242110 (2011).
[6] H. Y. Kim, J. H. Kim, Y. J. Kim, Optical Materials. **17**, 141 (2001).
[7] Hongxia Qi, Qingshan Li, Caifeng Wang, Vacuum. **81**, 943 (2007).
[8] Lung Chien Chen, Mo-Inn Lu, Scripta Materialia. **61**, 781 (2009).
[9] J. Y. Lee, Y. S. Choi, J. H. Kim, Thin Solid Films. **420**, 112 (2002).
[10] Kyeongmi Lee, Kenji Nomura, Hiroshi Yanagi, J. Appl. Phys. **112**, 033713 (2012).
[11] Min-Suk Oh, Sang-Ho Kim, Tae-Yeon Seong, APL. **87**, 122103 (2005).
[12] Chia-Chin Huang, Jalin Ko-Tsung Huang, Chi-Wei Lee, IEEE Sensor Journal. **12**, 1289 (2012).
[13] Tsung-Hsun Tsai and Richard Hornsey, IEEE Sensor Journal. **1**, 1 (2012).
[14] Thomas L. Paoli, Peter A. Barnes, APL. **28**, 714 (1976).
[15] Tzu-Chiang Lin, Ta-Chun Ma, Hao-Hsiung Lin, IEEE Photonics Technology Letters, **20**, 1429 (2008).
[16] R. F. Wolffenbuttel, IEEE Electron Device Lett. EDL-8, 13 (1987).
[17] M. Fernandes, Yu. Vygranenko, R. Schwarz, Sensors and Actuators A. **92**, 152 (2001).
[18] Guo-Tong Du, Wang Zhao, Guo-Guang Wu, APL. **101**, 053503 (2012).
[19] Bigas, M. Cabruja, E., Forest, J., Salvi, J., Microelectronics J. **37**, 433 (2006).
[20] Tsung-Hsun Tsai, Richard Hornsey, IEEE Sensors Journal, **12**, 3277 (2012).
[21] Sung-Hyun Jo, Myunghan Bae, Pyung Choi, IEEE International Conference on Computer Science and Automation Engineering (CSAE) **3**, 363 (2012).

*Corresponding author: ZGL.semicon@gmail.com